NUCL SCI TECH (2020) 31:21
https://doi.org/10.1007/s41365-020-0724-x

Stability study of Disperse Blue 79 under ionizing radiation

Xiao-Jun Ding[1,2] · Ming Yu[3] · Xin Zheng[1] · Cui-Cui Ye[1] · Yu Gu[1] · Man-Li Lu[1] · Bo-Wu Zhang[3] · Lin-Fan Li[1] · Jing-Ye Li[1,3]

Received: 6 October 2019 / Revised: 17 November 2019 / Accepted: 3 December 2019 / Published online: 8 February 2020

Abstract Ionizing radiation is a promising method for dye degradation or textile coloration using commercial azo dyes and small molecular weight organic dyes. Thus, the stability of the molecular structure of an azo dye is important under ionizing radiation. Disperse Blue 79, as an example azo dyes, was irradiated with gamma rays or electron beam (EB) to investigate the radiation-induced effects on the molecular structure. Ultraviolet visible spectroscopy (UV–Vis), nuclear magnetic resonance (NMR) spectra analysis, and mass spectrometry (MS) studies indicated that acetoxy and methoxyl were easily cleaved on the irradiation of the aqueous dye solution but retained a stable structure on the irradiation of the powder form. Gamma rays and EB showed similar effects on the decomposition process. Chromaticity changes using the *Lab** method showed that the dye turned to dark yellow and the value of *b** of the irradiated dyes increased with the increasing absorbed dose, which indicated that Disperse Blue 79 could be partly decomposed in an aqueous solution with an absorbed dose of 10 kGy. Furthermore, the results demonstrated that the chemical stability of the Disperse Blue 79 under ionizing radiation are different in its powder form with the dye in the aqueous solution.

Keywords Azo dyes · Disperse Blue 79 · Stability · Irradiation

1 Introduction

Azo dyes constitute nearly half of the organic dyes used in the dyeing industry. Azo dyes consist of monoazo, diazo, and triazo classes, among which 70% are monoazo [1]. Azo dyes are widely used in the conventional dyeing process and new dyeing methods involving supercritical dyeing technology [2] and as dyes related to functional applications [3–5]. Environmental and human health issues caused by the extensive azo dye usage have promoted researches involving decolorization and degradation of the azo dyes from dyeing wastewater by methods including adsorption [6–8], biocoagulation [9], and catalysis [10]. For example, SEN et al. [11] reviewed fungal decoloration and degradation of azo dyes and reported that the fungal decoloration mechanism mainly includes adsorption and enzymatic degradation. Rapid oxidation physicochemical methods have also been proposed as effective means for dye wastewater treatment [12–16].

Ionizing radiation is a method using high-energy rays or charged particles to induce the formation of ions, excited molecules, and free radicals in water and organic molecules. Types of ionizing radiation include gamma ray, electron beam (EB), and ultraviolet (UV) radiation. For example, UV radiation is important for plant growth and

This work was financially supported by the National Natural Science Foundation of China (Nos. 11875313, 11605274, and 11575277).

Xiao-Jun Ding and Ming Yu contributed equally to this work.

✉ Jing-Ye Li
jyli@shnu.edu.cn

[1] Shanghai Institute of Applied Physics, Chinese Academy of Sciences, Shanghai 201800, China

[2] University of Chinese Academy of Sciences, Beijing 100049, China

[3] The Education Ministry Key Lab of Resource Chemistry, Shanghai Key Lab of Rare Earth Functional Materials, College of Chemistry and Materials Science, Shanghai Normal University, Shanghai 200234, China

metabolism [17]. However, overexposure to UV radiation will break chemical bonds and cause severe health problems [18]. Molecular structures can be broken and new chemical bonds formed during ionizing radiation exposure [19]. Therefore, changes in the molecular structure under ionization radiation must be analyzed considering that ionizing radiation has been reported as an effective means for dye degradation [20, 21], textile coloration [22], and fabric functionalization [23, 24]. In high-energy radiation-induced coloration or degradation processes, dyes are placed under radiation to generate radicals, which inevitably influence the dye's chemical structure. Therefore, understanding the structural stability of azo dyes under ionizing radiation is vital. During decolorization, azo dyes have been reported to release aniline groups, which are carcinogenic and harmful to human health and ecological balance [11, 25]. However, changes in chemical structures during reduction and decoloration have not attracted extensive attention [26]. Porobić et al. [27] synthesized a pyridone azo dye, investigated its thermal decomposition mechanism and found the relationship between thermal stabilities and chemical structures of the dye. Kiayi et al. [28] used *Saccharomyces cerevisiae* to degrade carmoisine and demonstrated that azo dyes are degraded into aromatic amines. Mu et al. [29] found that AO7 is cleaved into sulfanilic acid and 1-amino-2-naphthol by irradiation. However, changes in the azo dye molecular structure by ionizing radiation have not been extensively reported. Among azo dyes, Disperse Blue 79, a monoazo, has been widely produced and used in polyester [30] and other textile applications [31], therefore, the radiation-induced molecular structural changes of Disperse Blue 79 could be regarded as a representative for the azo dyes. Weber et al. [1] reported the chemical reduction in Disperse Blue 79 in a water system and demonstrated that Disperse Blue 79 results in 2-bromo-4,6-dinitroaniline. Hou [32] investigated the crystal morphology of Disperse Blue 79. However, till date, structural changes of Disperse Blue 79 under ionizing radiation have not been reported.

Gamma rays or EB are commonly used ionizing radiation sources. Gamma rays have high penetrability ($\geq$ 10 cm in water) but a low dose rate ($\leq$ 10 kGy•h^{-1}), while EB has a high dose rate (5 kGy•s^{-1}) but low penetrability ($\leq$ 5 mm in water). Both can generate ions and radicals and result in changes in the molecular structure of a compound [33]. This study focused on the molecular structural stability of Disperse Blue 79 irradiated by gamma rays and EB. Pure Disperse Blue 79 in aqueous solution, prepared by dissolving in deionized water, or its powder form was irradiated by gamma rays or EB. Moreover, commercial Disperse Blue 79 in aqueous solution and powder form was irradiated by gamma rays and EB. Changes in the chemical structure were characterized by UV–Vis, NMR, and mass spectrometry to clarify the structural differences between dyes in aqueous solution and powder irradiated by gamma rays and EB. The effects of the absorbed dose on the structures and properties of the dyes were studied. *Lab** values of the dyes were measured to study chromaticity variations arising due to different absorbed doses and radiation types.

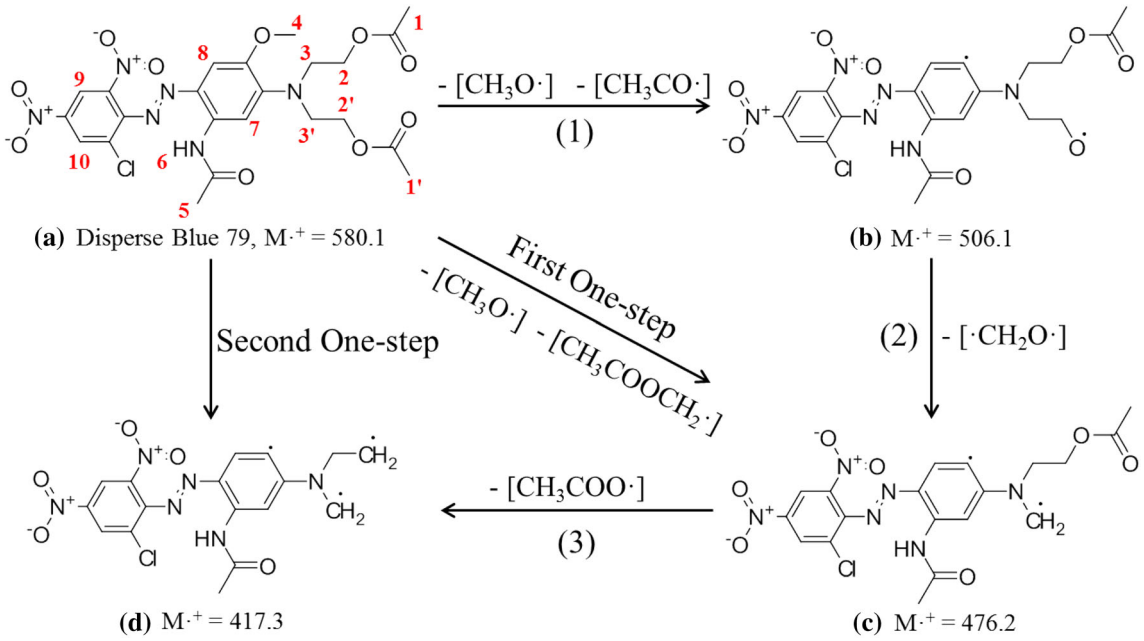

Scheme 1. Decomposition process of Disperse Blue 79

2 Experimental section

2.1 Chemicals and instruments

Commercial Disperse Blue 79 was obtained from Zhejiang Greenland Textile Technology Co., Ltd. (Wenzhou, China). Pure Disperse Blue 79 (99% pure) was purchased from Sinopharm Chemical Reagent Co., Ltd. (Shanghai, China). The cotton fabric of GB/T7568.2-2008 was obtained from the Shanghai Textile Industry Institute of Technical Supervision (Shanghai, China). All reagents were used without further purification.

*Lab** values of the samples were measured using a colorimeter (NR10QC, 3nh, Shenzhen, China). Mass spectrometry was conducted on an Agilent QTOF 6540 instrument (Agilent Technologies, Inc., Santa Clara, CA, USA) in deionized water with an electrospray ionization interface (ESI), and data were analyzed by the MestReNova software (Mestrelab Research S.L.). NMR spectrometry was performed on an Avance 500 instrument (Bruker Corp., Billerica, MA, USA) with 500 MHz in deuterated dimethylsulfoxide (DMSO-d6), at a concentration of 4 g/L; data were analyzed by MestReNova. UV–Vis spectrometry was performed on a UV-3010 spectrophotometer (Mettler-Toledo International Inc., Greifensee, Switzerland) in the range of 200–800 nm in deionized water.

2.2 Dye irradiation

2.2.1 Gamma-ray irradiation

The Disperse Blue 79 powder was dissolved in deionized water to a concentration of 10 g/L in a glass bottle and ultrasonicated for 5 min to accelerate dissolution. The solutions were irradiated under a ^{60}Co gamma-ray source for 17 h with the absorbed doses of 10, 50, or 150 kGy. The irradiated solutions were placed into a vacuum oven for water removal at 60 °C. Powder irradiation was performed by placing 1 g of the dye powder in a polythene bag directly under the gamma-ray source.

2.2.2 EB irradiation

The Disperse Blue 79 powder was dissolved in deionized water with a concentration of 10 g/L in a polythene

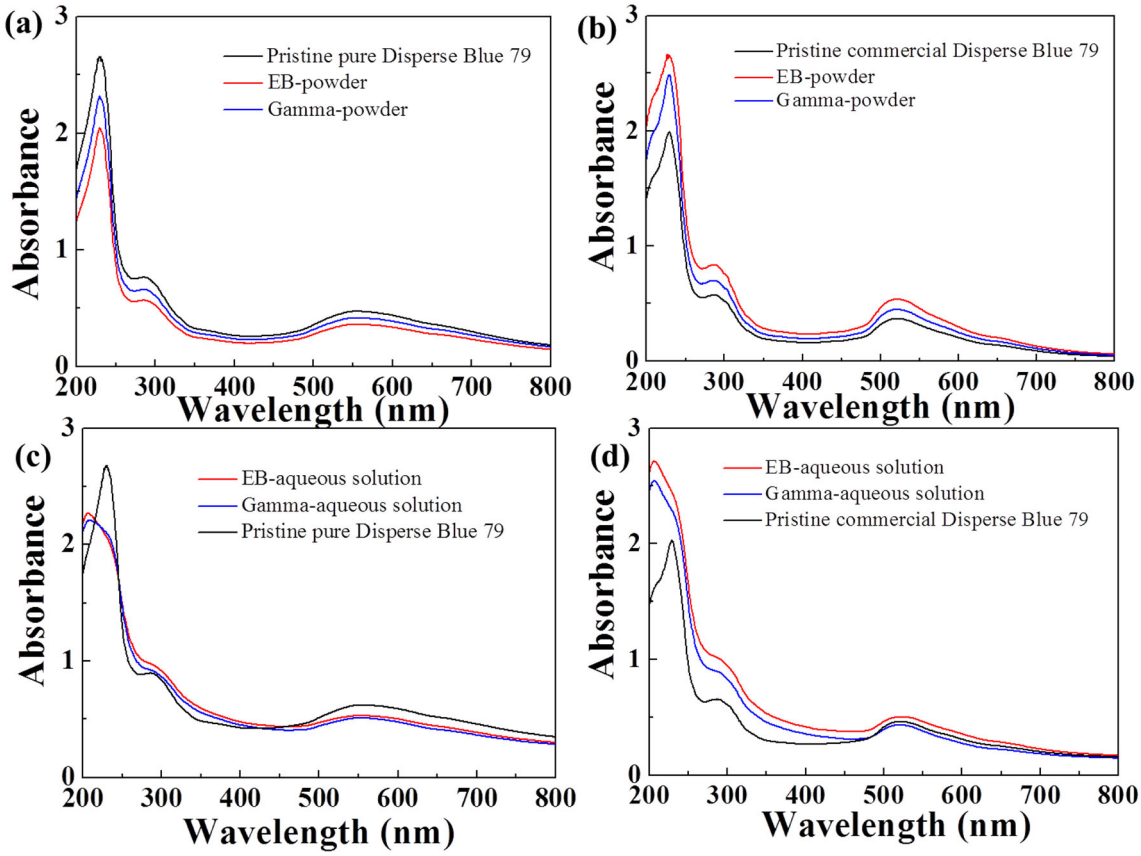

Fig. 1 (Color online) UV–Vis spectra of **a** pure, **b** commercial Disperse Blue 79 irradiated by gamma rays and EB in powder form, and **c** pure, **d** commercial Disperse Blue 79 irradiated by gamma rays and EB in aqueous solution

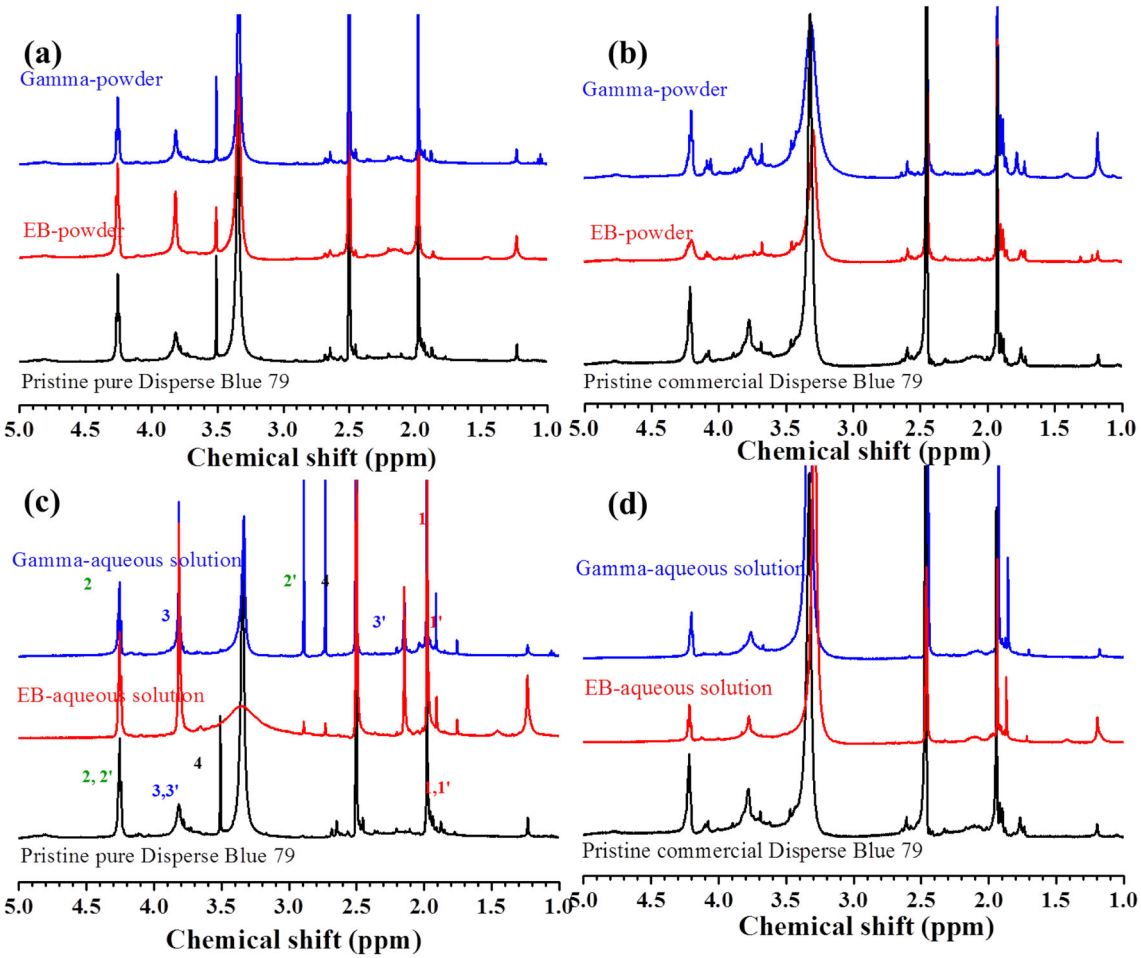

Fig. 2 (Color online) ^{1}H NMR spectra of **a** pure, and **b** commercial Disperse Blue 79 irradiated by gamma rays and EB in powder form, and **c** pure, and **d** commercial Disperse Blue 79 irradiated by gamma rays and EB in aqueous solution

bag and ultrasonicated for 5 min to accelerate dissolution. The sample bags were placed under a 1.2 MeV electron accelerator for irradiation with an absorbed dose of 10, 50, or 150 kGy. The irradiated solutions were placed into a vacuum oven for water removal at 60 °C. Powder irradiation was performed by placing 1 g of the dye powder in a polythene bag directly under the EB source.

3 Results and discussion

3.1 Irradiation of Disperse Blue 79

Commercial dyes usually contain additives [34, 35], including dispersants and diluents. And the same-class dyes with different chemical structures are mixed in various proportions by dye manufacturers. The structure of the pure Disperse Blue 79 is shown in Scheme 1. The halogen substituent and alkyl groups could be varied during synthesis by manufacturers to obtain desired properties including temperature and pH sensitivities, solubility in defined solvents, compatibility with fabric, and thermal stability. Thus, it is necessary to investigate radiation-induced effects on both commercial and pure Disperse Blue 79. Water is a common solvent for dye dissolution and reaction. Pure and commercial Disperse Blue 79 dye powders were dissolved in water and irradiated with gamma rays or EB at absorbed doses of 150 kGy to study

Table 1 Pristine pure Disperse Blue 79 ^{1}H-NMR (DMSO-d6) spectra data from Fig. 2c

δH/ppm (J/Hz)	H	Assignment
1.98(s)	CH_3, CH_3	1,1’
1.81–2.02(s)	CH_3	5
3.51(s)	CH_3	4
3.82(t)	CH_3, CH_2	3,3’
4.25(t, ^{3}J/6.1)	CH_2, CH_2	2,2’

dye structural changes occurring due to the decomposition [36, 37] and radical formation [38, 39] that were induced by ionizing radiation of water. Also, pure and commercial Disperse Blue 79 powders were irradiated directly by gamma rays or EB with absorbed doses of 150 kGy to investigate the influence of radiation on dyes during solid-phase radiation-induced applications.

3.2 Characterization and analysis of decomposition

3.2.1 UV–Vis study

UV–Vis spectra showed that there were no significant peak changes for pure and commercial Disperse Blue 79 powders undergoing direct irradiation (Fig. 1a, b). The observed difference was that λ_{max} characteristic peaks of the azo aromatic chromophore [40, 41] of the commercial dye exhibited a hypsochromic shift as compared with that of the pure dye. Notably, the absorption peak of pure and commercial dyes in aqueous solution at 228 nm significantly decreased while that at 210 nm increased after gamma-ray and EB irradiation (Fig. 1c, d). This indicated that there were cleavages and formation of higher energy electronic transition structures, such as C–H and C–C bonds [42]. These spectra indicated that both dyes experienced structural changes when irradiated in aqueous solution by gamma rays and EB but remained stable in the powder form.

3.2.2 NMR study

^{1}H-NMR spectra of Disperse Blue 79 dyes irradiated with an absorbed dose of 150 kGy are shown in Fig. 2, and the detailed data of the pristine pure dye listed in Table 1. Each site of C and related H are marked in Scheme 1. Except for water and DMSO peaks at 2.5 and 3.4 ppm, the 5 site related to the methyl group at the end of amide did not show a distinct single peak from 1.8 to 2.0 ppm (Fig. 2a). Similarly, 3 and 3′ sites related to methylene adjacent to a tertiary amine also merely showed a single weak peak at 3.82 ppm. In the commercial Disperse Blue 79, methoxyl group did not show a distinct peak (Fig. 2b). The dyes in powder form irradiated with absorbed doses of 150 kGy maintained their original peaks, similar to the pristine dyes of both commercial and pure Disperse Blue 79 under gamma-ray and EB irradiation (Fig. 2a, b), which confirmed that the Disperse Blue 79 powder successfully resisted gamma-ray and EB irradiation, as confirmed by UV–Vis analysis. The NMR spectra of pure Disperse Blue 79 in aqueous solution irradiated by gamma rays and EB with the absorbed dose of 150 kGy are shown in Fig. 2c. The peak area changes were calculated and compared to confirm the decomposition by ensuring same concentrations in DMSO-d6. It was found that methyl at the 1′ and 1 as well as at 2′ and 3′ sites split to two peaks. Furthermore, methoxyl at the 4 site shifted. The peak area changes indicated that methoxyl and acetoxy methyl groups of pure

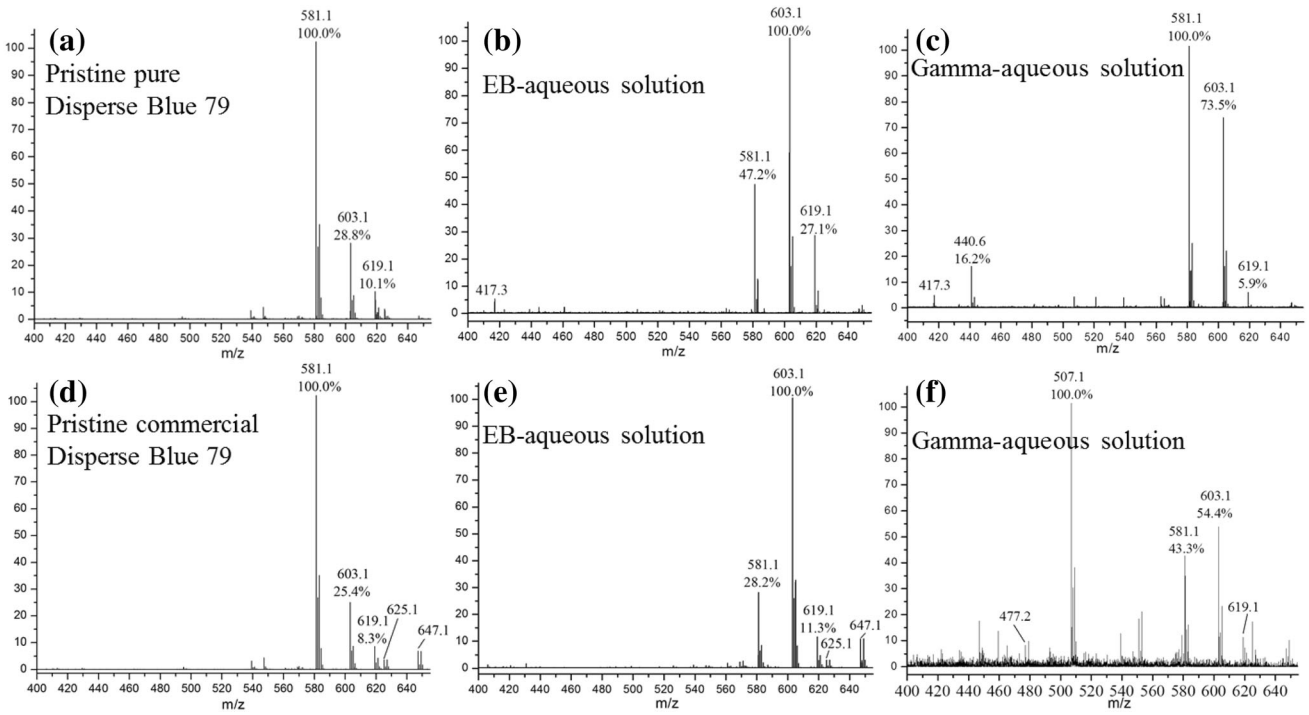

Fig. 3 Mass spectra of **a**, **b**, **c** pure and **d**, **e**, **f** commercial Disperse Blue 79 irradiated by gamma rays and EB in aqueous solution

Disperse Blue 79 were decomposed in aqueous solution, which is illustrated as the "First One-step" decomposition process in Scheme 1. The commercial Disperse Blue 79 in aqueous solution experienced the same degradation paths when irradiated by gamma rays and EB. The split peak at the 1′ site was identical to that observed for the pure dye (Fig. 2d). Thus, ^{1}H-NMR spectra demonstrated that pure and commercial Disperse Blue 79 experienced the "First One-step" decomposition process when irradiated in aqueous solution and maintained stable structures when irradiated in powder form.

3.2.3 Mass spectrometry study

The mass spectra of pure and commercial Disperse Blue 79 irradiated in aqueous solution are shown in Fig. 3. The mass-to-charge ratio of the newly formed ion at 417 for pure Disperse Blue 79 in aqueous solution irradiated with gamma rays and EB (Fig. 3a–c) indicated that another carboxyl group had decomposed (step_3) on the basis of the First One-step decomposition process concluded from the NMR results. This path is illustrated as the "Second One-step" degradation process in Scheme 1. In the commercial Disperse Blue 79 mass spectra (Fig. 3d–f), there were no distinct new peaks in aqueous solution of EB-irradiated dyes, but decreased intensity of the main structure was observed. However, a distinct mass-to-charge ratio at 507 in gamma-ray-irradiated aqueous dyes revealed that the methoxyl and acetyl groups were likely degraded (step_1). Also, a mass-to-charge ratio at 477 demonstrated that fragments at 507 could experience further degradation by splitting a methoxyl group (step_2). Although Disperse Blue 79 partly in aqueous solution decomposed on irradiation, the main N=N bond of the azo molecule resisted irradiation. This means that the methoxyl and acetyl groups were more easily attacked than the C–N and N=N bonds in the azo molecule by reactive radicals generated in irradiated water, which showed different cleavage pathways that

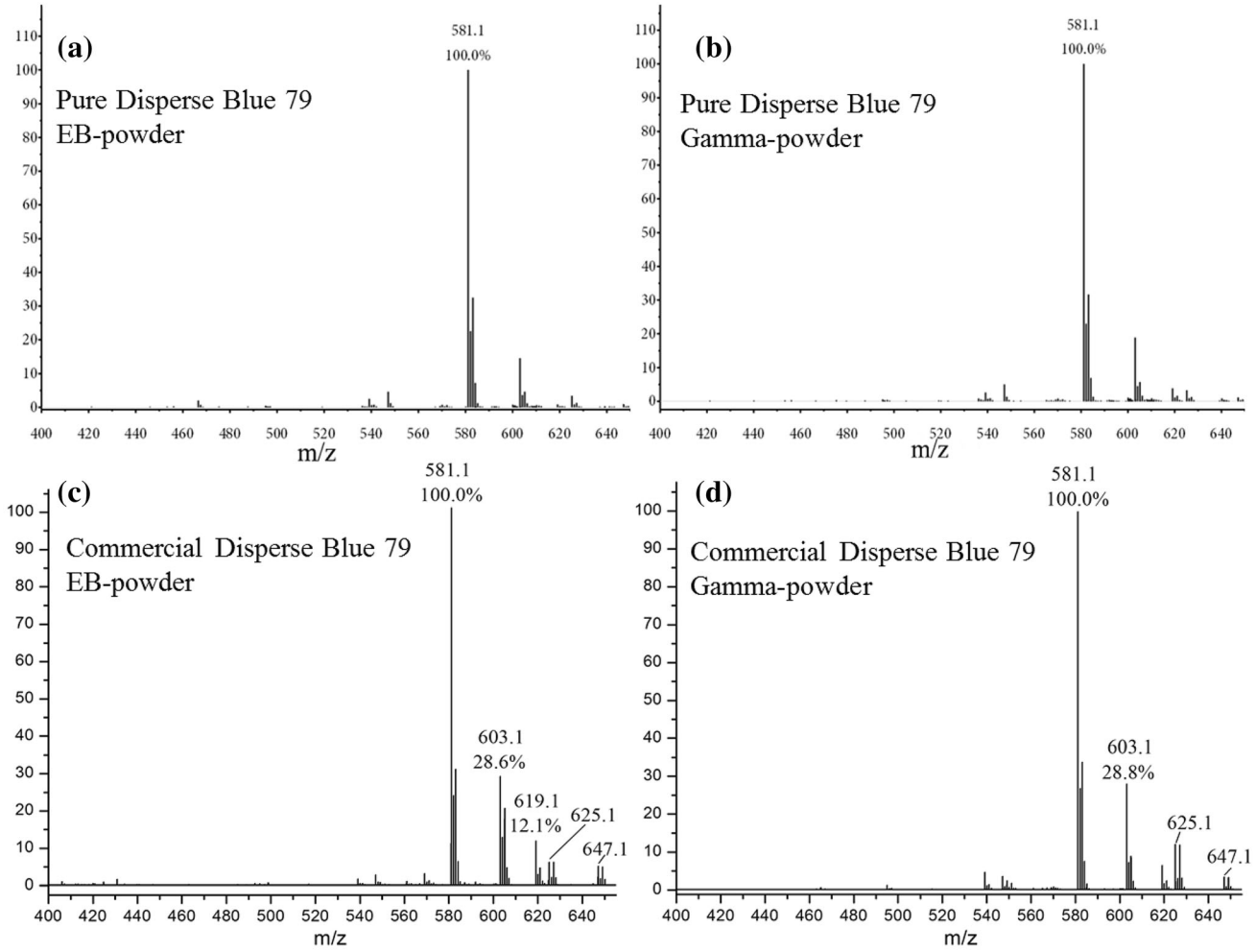

Fig. 4 Mass spectra of pure Disperse Blue 79 irradiated by **a** EB and **b** gamma rays and commercial Disperse Blue 79 irradiated by **c** EB and **d** gamma rays in powder form

Table 2 Mass spectrometry data of commercial and pure Disperse Blue 79

Formula	Calculated mass	Double bond equivalence	Adduct	Charge state	m/z
C_{23} H_{25} N_6 O_{10} Cl	580.1	14.0	H+	+ 1	581.1
			Na+	+ 1	603.1
			K+	+ 1	619.1
C_{20} H_{20} N_6 O_8 Cl	506.1	13.0	H+	+ 1	507.1
C_{19} H_{18} N_6 O_7 Cl	476.2	13.0	H+	+ 1	477.2
C_{17} H_{14} N_6 O_5	440.6	12.0	–	–	440.6
C_{17} H_{15} N_6 O_5 Cl	417.3	12.0	–	–	417.3
C_{23} H_{25} N_6 O_{10} Br	624.0	14.0	H+	+ 1	625.1
			Na+	+ 1	647.1

were previously reported [43]. The mass spectra of pure and commercial Disperse Blue 79 dyes irradiated in powder form are shown in Fig. 4. The detailed mass-to-charge ratios of the molecule are listed in Table 2. It was clearly observed that the pure (Fig. 4a, b) and commercial dyes (Fig. 4c, d) in powder form maintained stable structures, identical to pristine dyes (Fig. 3a, d), after irradiation. The results agreed with UV–Vis and NMR results. Furthermore, the mass-to-charge ratios at 625 and 647 in the commercial Disperse Blue 79 indicated that chlorine atom was partly replaced by bromine atom (Table 2), which further demonstrated that commercial products usually contain mixed dye compositions. The stability of Disperse Blue 79 in powder form revealed that oxygen in air did not have a distinct effect on the dyes [44] or form oxidized products [45, 46] during irradiation. Overall, the mass spectrometry results matched NMR and UV–Vis spectra and indicated that pure and commercial Disperse Blue 79 partly decomposed when irradiated in aqueous solution and were stable as powder under gamma-ray and EB irradiation. The pure dye mainly experienced the Second One-step process, while the commercial dye underwent a stepwise path. However, the decomposition paths of both dyes proved that acetoxy and methoxyl groups were easily decomposed under irradiation in aqueous solution.

3.3 Chromaticity effects of irradiated dyes

The investigation of chromaticity changes of the dyes is important for both dye degradation and coloration applications [47]. Herein, pure and commercial Disperse Blue 79 in aqueous solution and powder were irradiated while the absorbed dose was increased from 0 to 150 kGy. The irradiated dyes were diluted to 1 g/L and dripped on fabric surfaces to test color variations. The *Lab** method is commonly used to quantitatively define the chromaticity changes [47, 48], in which L^* value represents the luminosity, a^* represents the red/green opponent colors, and b^* represents the yellow/blue opponent colors. The results revealed that the chromaticity of pure Disperse Blue 79

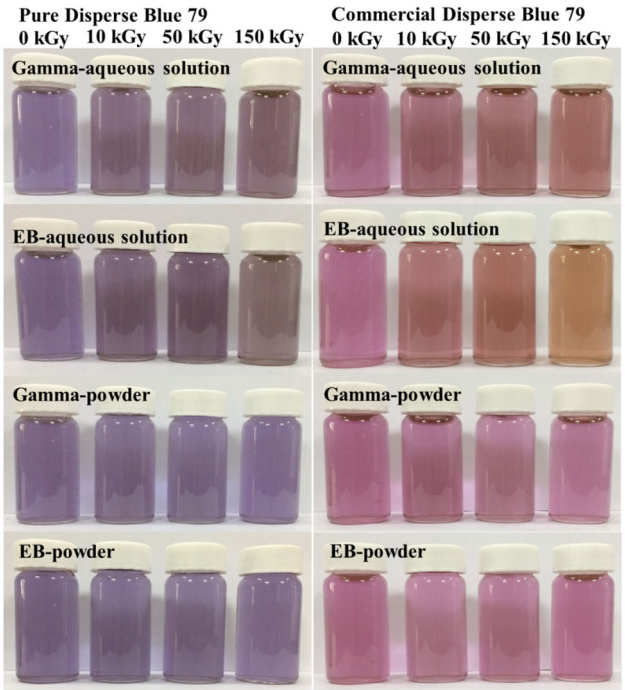

Fig. 5 (Color online) Pure and commercial Disperse Blue 79 irradiated by gamma rays and EB in aqueous solution and powder dissolved in deionized water (1 mg/L)

turned to dark yellow from original blue after irradiated by gamma rays and EB in aqueous solution (Fig. 5). Original blue deeply faded with the increased absorbed dose, which indicated that pure Disperse Blue 79 decomposed significantly with the increased absorbed dose. But, the color almost did not change after irradiated in powder. The commercial Disperse Blue 79 was also decomposed under irradiation in aqueous solution but maintained its original color in powder form. The values of a^* and b^* of the dyed fabric were measured to define the color changes of Disperse Blue 79. The results showed that for pure Disperse Blue 79, a^* was almost constant but b^* increased after irradiated in aqueous solution (Fig. 6a, b). The higher value of b^* indicated that the dye color turned from blue to yellow, which was in accordance with color changes shown

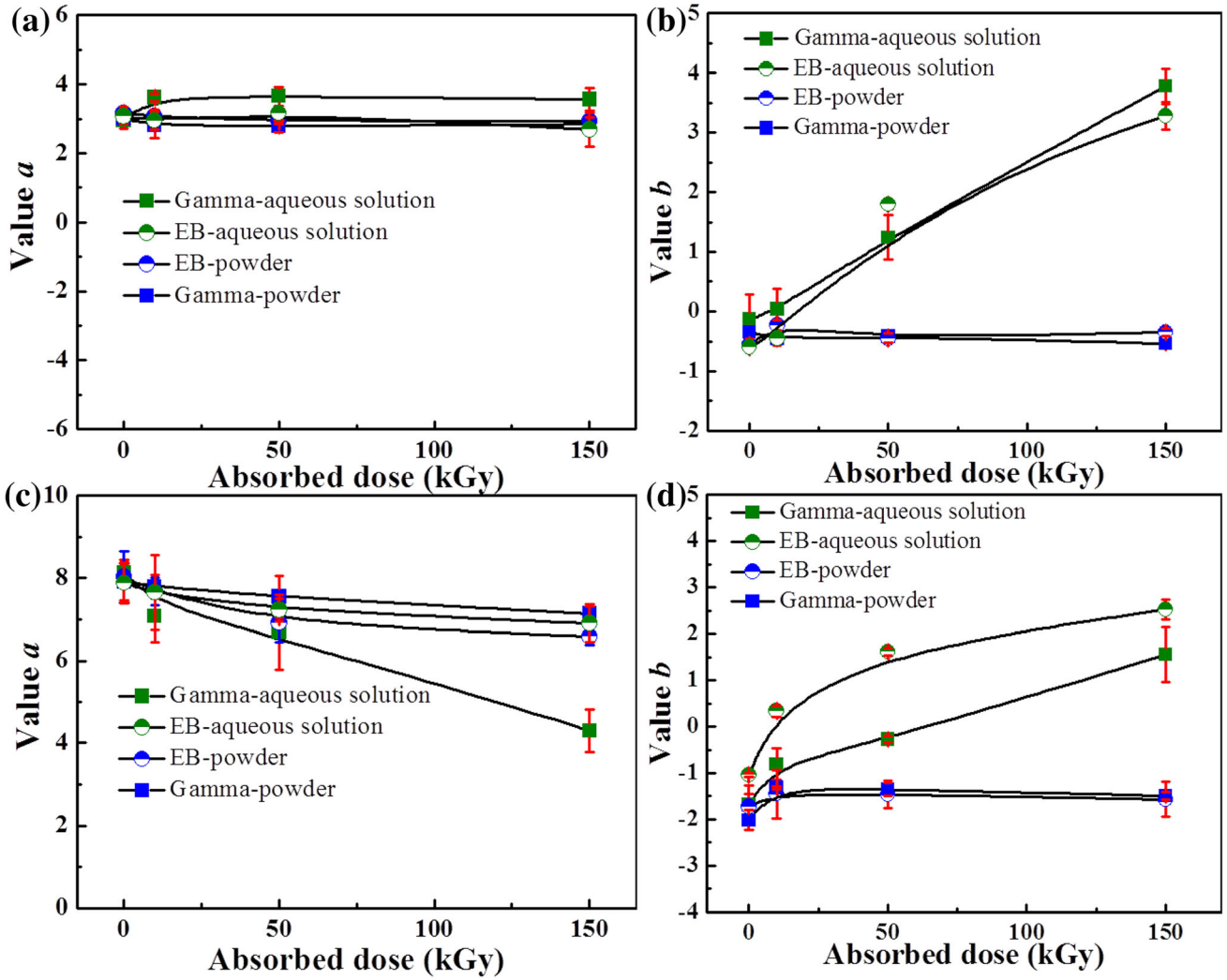

Fig. 6 (Color online) *Lab** method of value *a** and *b** of **a**, **b** pure and **c**, **d** commercial Disperse Blue 79 after irradiation

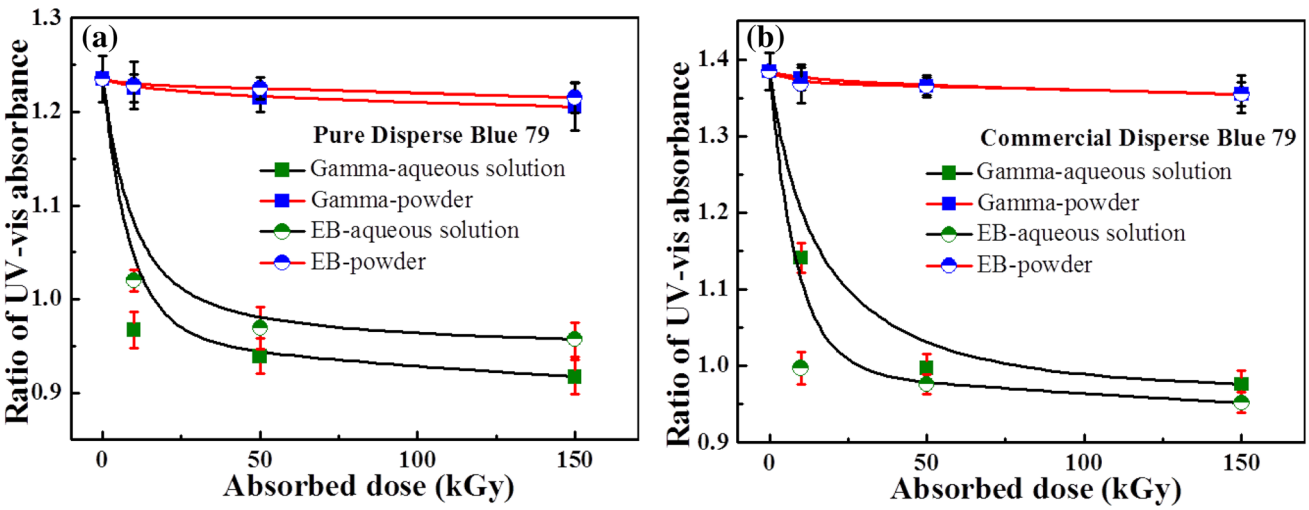

Fig. 7 (Color online) Ratio of UV–Vis absorption values ($Abs_{228\ nm}/Abs_{210nm}$) of **a** pure, **b** commercial Disperse Blue 79 in aqueous solution and powder form irradiated by gamma rays and EB with different absorbed doses

in Fig. 5. Notably, the commercial Disperse Blue 79 showed red color when dissolved in aqueous solution but similar chromaticity changes were observed with irradiation (Figs. 5, 6c, d). The chromaticity changes confirmed that commercial and pure Disperse Blue 79 in aqueous solution experienced structural changes under gamma-ray and EB irradiation but mostly maintained original structures in powder form under gamma-ray and EB irradiation at an absorbed dose of 150 kGy. In addition, the increased absorbed dose enhanced dye decomposition. Moreover, the results indicated that the decomposition of acetoxy and methoxyl groups could influence dye chromaticity.

3.4 Effects of absorbed doses on irradiated dyes

UV–Vis spectra of dyes in aqueous solution and powder irradiated with the absorbed dose of 0–150 kGy were measured to investigate the effect of the absorbed doses. The absorption values at 228 and 210 nm were calculated to compare peak area changes (Fig. 7). The results showed that pure and commercial dyes in aqueous solution undergo structural changes under gamma-ray and EB irradiation with an absorbed dose of 10 kGy and remained balanced over 50 kGy, indicating low absorbed dose effects on irradiation [49]. In contrast, the dyes in powder form were stable at all doses. The results indicated that both dyes could be decomposed with a relatively low absorbed dose, which indicated the instability of Disperse Blue 79 when irradiated in aqueous conditions.

4 Conclusion

Pure and commercial Disperse Blue 79 in aqueous solutions were irradiated by gamma rays and EB to investigate the effect of irradiation on the dye structure. Moreover, dyes in powder form were irradiated to study the influence of air. UV–Vis spectra showed that pure and commercial Disperse Blue 79 in aqueous solution experienced structural changes when irradiated by gamma rays and EB but notably remained stable in powder form. NMR results indicated that the structural change of pure Disperse Blue 79 could be attributed to the First One-step decomposition path. Mass spectrometry results demonstrated that under irradiation of pure Disperse Blue 79, carboxyl groups were decomposed or directly underwent the "Second One-step," but the commercial Disperse Blue 79 experienced stepwise decomposition paths by splitting methoxyl and acetyl groups at step_1 and another methoxyl at step_2. All results indicated that gamma rays and EB have almost the same effect on the dye structure. Furthermore, chromaticity analysis showed that the color of Disperse Blue 79 turned to dark yellow when irradiated in aqueous solution and maintained its original color (blue) when irradiated in powder form. The dispersed dye was extremely unstable in aqueous solution when irradiated by gamma rays and EB with an absorbed dose of 10 kGy.

Acknowledgements The authors thank Zhejiang Greenland Textile Technology Co., Ltd. for the kind supply of Commercial Disperse Blue 79.

References

1. E.J. Weber, R.L. Adams, Chemical and sediment-mediated reduction of the Azo dye disperse blue 79. Environ. Sci. Technol. **29**, 1163–1170 (1995). https://doi.org/10.1021/es00005a005
2. F. Li, L. Lv, X. Wang et al., Constructhttps://doi.org/10.1021/acssuschemeng.8b03976ing of dyes suitable for eco-friendly dyeing wool fibers in supercritical carbon dioxide. ACS Sustain. Chem. Eng. **6**, 16726–16733 (2018).
3. A. Aboelnaga, S. Shaarawy, A.G. Hassabo, Polyaconitic acid/functional amine/azo dye composite as a novel hyper-branched polymer for cotton fabric functionalization. Colloids Surfaces B. Biointerfaces. **172**, 545–554 (2018). https://doi.org/10.1016/j.colsurfb.2018.09.012
4. J.-H. Park, U.-Y. Kim, B.-M. Kim et al., Molecular design strategy toward robust organic dyes in thin-film photoanodes. ACS Appl. Energy Mater. **2**, 4674–4682 (2019). https://doi.org/10.1021/acsaem.8b02100
5. A. Villela, M.S.A. van Vuuren, H.M. Willemen et al., Photostability of a flavonoid dye in presence of aluminium ions. Dyes Pigments. **162**, 222–231 (2019). https://doi.org/10.1016/j.dyepig.2018.10.021
6. P. Huang, D. Xia, A. Kazlauciunas et al., Dye-mediated interactions in chitosan-based polyelectrolyte/organoclay hybrids for enhanced adsorption of industrial dyes. ACS Appl. Mater. Interface. **11**, 11961–11969 (2019). https://doi.org/10.1021/acsami.9b01648
7. Z. Liu, L. Zhang, F. Dong et al., Preparation of ultrasmall goethite nanorods and their application as heterogeneous fenton reaction catalysts in the degradation of Azo dyes. ACS Appl. Nano Mater. **1**, 4170–4178 (2018). https://doi.org/10.1021/acsanm.8b00930
8. M. Vall, M. Strømme, O. Cheung, Amine-modified mesoporous magnesium carbonate as an effective adsorbent for Azo dyes. ACS Omega. **4**, 2973–2979 (2019). https://doi.org/10.1021/acsomega.8b03493
9. M. Chethana, L.G. Sorokhaibam, V.M. Bhandari et al., Green approach to dye wastewater treatment using biocoagulants. ACS Sustain. Chem. Eng. **4**, 2495–2507 (2016). https://doi.org/10.1021/acssuschemeng.5b01553
10. S.L. Shinde, K.K. Nanda, Photon-free degradation of dyes by Ge/GeO_2 porous microstructures. ACS Sustain. Chem. Eng. **7**, 6611–6618 (2019). https://doi.org/10.1021/acssuschemeng.8b05549
11. S.K. Sen, S. Raut, P. Bandyopadhyay et al., Fungal decolouration and degradation of azo dyes: a review. Fungal Biol. Rev. **30**, 112–133 (2016). https://doi.org/10.1016/j.fbr.2016.06.003
12. S. Martínez-López, C. Lucas-Abellán, A. Serrano-Martínez et al., Pulsed light for a cleaner dyeing industry: Azo dye degradation by an advanced oxidation process driven by pulsed light. J. Clean. Prod. **217**, 757–766 (2019). https://doi.org/10.1016/j.jclepro.2019.01.230

13. I.I. Raffainer, P. Rudolf von Rohr, Promoted wet oxidation of the Azo dye orange II under mild conditions. Ind. Eng. Chem. Res. **40**, 1083–1089 (2001). https://doi.org/10.1021/ie000629a
14. L. Szpyrkowicz, C. Juzzolino, S.N. Kaul, S. Daniele et al., Electrochemical oxidation of dyeing baths bearing disperse dyes. Ind. Eng. Chem. Res. **39**, 3241–3248 (2000). https://doi.org/10.1021/ie9908480
15. H. Wang, W. Zhang, J. Zhao et al., Rapid decolorization of phenolic Azo dyes by immobilized laccase with Fe_3O_4/SiO_2 nanoparticles as support. Ind. Eng. Chem. Res. **52**, 4401–4407 (2013). https://doi.org/10.1021/ie302627c
16. L. Szpyrkowicz, R. Cherbanski, G.H. Kelsall, Hydrodynamic effects on the performance of an electrochemical reactor for destruction of disperse dyes. Ind. Eng. Chem. Res. **44**, 2058–2068 (2005). https://doi.org/10.1021/ie049444k
17. X. Li, M. Ma, W. Shao et al., Molecular cloning and functional analysis of a UV-B photoreceptor gene, BpUVR8 (UV Resistance Locus 8), from birch and its role in ABA response. Plant Sci. **274**, 294–308 (2018). https://doi.org/10.1016/j.plantsci.2018.06.006
18. X.X. Feng, L.L. Zhang, J.Y. Chen et al., New insights into solar UV-protective properties of natural dye. J. Clean. Prod. **15**, 366–372 (2007). https://doi.org/10.1016/j.jclepro.2005.11.003
19. R. Miraftab, B. Ramezanzadeh, G. Bahlakeh, An advanced approach for fabricating a reduced graphene oxide-AZO dye/polyurethane composite with enhanced ultraviolet (UV) shielding properties Experimental and first-principles QM modeling. Chem. Eng. J. **321**, 159–174 (2017). https://doi.org/10.1016/j.cej.2017.03.124
20. I. Shahidul, F. Mohammad, High-energy radiation induced sustainable coloration and functional finishing of textile materials. Ind. Eng. Chem. Res. **54**, 3727–3745 (2015). https://doi.org/10.1021/acs.iecr.5b00524
21. M. Yu, W. Li, Z. Wang et al., Covalent immobilization of metal-organic frameworks onto the surface of nylon-a new approach to the functionalization and coloration of textiles. Sci Rep. **6**, 22796 (2016). https://doi.org/10.1038/srep22796
22. N.M. Mallikarjuna, J. Keshavayya, Synthesis, spectroscopic characterization and pharmacological studies on novel sulfamethaxazole based azo dyes. J. King Saud Univ. Sci. **32**, 251–259 (2018). https://doi.org/10.1016/j.jksus.2018.04.033
23. X. Ding, M. Yu, Z. Wang et al., A promising clean way to textile colouration: cotton fabric covalently-bonded with carbon black, cobalt blue, cobalt green, and iron oxide red nanoparticles. Green Chem. **21**, 6611–6621 (2019). https://doi.org/10.1039/C9GC02084E
24. X. Xu, X.J. Ding, J.X. Ao et al., Preparation of amidoxime-based PE/PP fibers for extraction of uranium from aqueous solution. Nucl. Sci. Tech. **30**, 20 (2019). https://doi.org/10.1007/s41365-019-0543-0
25. R.G. Saratale, G.D. Saratale, J.S. Chang et al., Bacterial decolorization and degradation of azo dyes: a review. J. Taiwan Inst. Chem. Eng. **42**, 138–157 (2011). https://doi.org/10.1016/j.jtice.2010.06.006
26. T. Suzuki, S. Timofei, L. Kunrunczi et al., Correlation of aerobic biodegradability of sulfonated azo dyes with the chemical structure. Chemosphere **45**, 1–9 (2001). https://doi.org/10.1016/s0045-6535(01)00074-1
27. S.J. Porobić, A.D. Krstić, D.J. Jovanović et al., Synthesis and thermal properties of arylazo pyridone dyes. Dyes Pigments. **170**, 107602 (2019). https://doi.org/10.1016/j.dyepig.2019.107602
28. Z. Kiayi, T.B. Lotfabad, A. Heidarinasab et al., Microbial degradation of azo dye carmoisine in aqueous medium using *Saccharomyces cerevisiae* ATCC 9763. J. Hazard. Mater. **373**, 608–619 (2019). https://doi.org/10.1016/j.jhazmat.2019.03.111
29. Y. Mu, K. Rabaey, R.A. Rozendal et al., Decolorization of Azo dyes in bioelectrochemical systems. Environ. Sci. Technol. **43**, 5137–5143 (2009). https://doi.org/10.1021/es900057f
30. J. Qiu, J. Xiao, B. Tang et al., Facile synthesis of novel disperse azo dyes with aromatic hydroxyl group. Dyes Pigments. **160**, 524–529 (2019). https://doi.org/10.1016/j.dyepig.2018.08.052
31. A.D. Broadbent, Y. Mir, M. Lhachimi et al., Continuous dyeing of cotton/polyester and polyester fabrics with reactive and disperse dyes using infrared heat. Ind. Eng. Chem. Res. **46**, 2710–2714 (2007). https://doi.org/10.1021/ie0700617
32. A. Hou, J. Dai, The crystal morphology of C.I. Disperse Blue 79 in supercritical carbon dioxide. Dyes Pigments. **82**, 71–75 (2009). https://doi.org/10.1016/j.dyepig.2008.11.004
33. H. Wang, L. Li, J. Guan et al., Investigation on molecular structures of electron-beam-irradiated low-density polyethylene by rheology measurements. Ind. Eng. Chem. Res. **57**, 4298–4310 (2013). https://doi.org/10.1021/acs.iecr.8b00062
34. R.R. Mather, Aggregate structures of samples of the disperse dye, C.I. Disperse Blue 79. Colloids Surf **37**, 131–140 (1989). https://doi.org/10.1016/0166-6622(89)80112-x
35. K.-M. Park, I. Yoon, S. Lee et al., X-ray crystal structure of C.I. Disperse Blue 79. Dyes Pigments **54**, 155–161 (2002). https://doi.org/10.1016/s0143-7208(02)00037-2
36. M. Wang, R. Yang, W. Wang et al., Radiation-induced decomposition and decoloration of reactive dyes in the presence of H_2O_2. Radiat. Phys. Chem. **75**, 286–291 (2006). https://doi.org/10.1016/j.radphyschem.2005.08.012
37. J.T. Spadaro, L. Isabelle, V. Renganathan, Hydroxyl radical mediated degradation of Azo dyes evidence for benzene generation. Environ. Sci. Technol. **28**, 1389–1393 (1994). https://doi.org/10.1021/es00056a031
38. J.E. Silveira, A.L. Garcia-Costa, T.O. Cardoso et al., Indirect decolorization of azo dye Disperse Blue 3 by electro-activated persulfate. Electrochim. Acta. **258**, 927–932 (2017). https://doi.org/10.1016/j.electacta.2017.11.143
39. J. Wu, W. Wen, Catalyzed degradation of Azo dyes under ambient conditions. Environ. Sci. Technol. **44**, 9123–9127 (2010). https://doi.org/10.1021/es1027234
40. A. Jabbar, A. Ambreen, S. Riaz et al., A series of new acid dyes; study of solvatochromism, spectroscopy and their application on wool fabric. J. Mol. Struct. **1195**, 161–167 (2019). https://doi.org/10.1016/j.molstruc.2019.05.019
41. L.C. Abbott, S.N. Batchelor, J.N. Moore, Structure and reactivity of thiazolium azo dyes: UV–visible, resonance Raman, NMR, and computational studies of the reaction mechanism in alkaline solution. J. Phys. Chem. A **117**, 1853–1871 (2013). https://doi.org/10.1021/jp309536h
42. C.C. Hsueh, B.Y. Chen, Exploring effects of chemical structure on azo dye decolorization characteristics by Pseudomonas luteola. J. Hazard. Mater. **154**, 703–710 (2008). https://doi.org/10.1016/j.jhazmat.2007.10.083
43. A.S. Ozen, V. Aviyente, Modeling the substituent effect on the oxidative degradation of Azo dyes. J. Phys. Chem. A. **108**, 5990–6000 (2004). https://doi.org/10.1021/jp037138z
44. E. Guerra, F. Gosetti, E. Marengo et al., Study of photostability of three synthetic dyes commonly used in mouthwashes. Microchem. J. **146**, 776–781 (2019). https://doi.org/10.1016/j.microc.2019.02.002
45. H.T. Wang, H.Q. Jiang, R.F. Shen et al., Electron-beam radiation effects on the structure and properties of polypropylene at low dose rates. Nucl. Sci. Tech. **29**, 87 (2018). https://doi.org/10.1007/s41365-018-0424-y
46. H.R. Tan, Z. Xing, W.H. Liu et al., Oxidation effects of poly (ether-ether-ketone) induced by electron-beam irradiation. J. Radiat. Res. Radiat. Process. **37**, 020201 (2019) (in Chinese). https://doi.org/10.11889/j.1000-3436.2019.rrj.37.020201

47. A.Y.L. Tang, C.H. Lee, Y.M. Wang et al., Reverse micellar dyeing of cotton fiber with reactive dyes: A study of the effect of water pH and hardness. ACS Omega. **4**, 11808–11814 (2019). https://doi.org/10.1021/acsomega.9b00597
48. W. Zheng, J. Zou, Synthesis and characterization of blue TiO2/CoAl2O4 complex pigments with good colour and enhanced near-infrared reflectance properties. RSC Adv. **5**, 87932–87939 (2015). https://doi.org/10.1039/c5ra17418j
49. Y.Y. Xie, Z.L. Chen, Z.L. Li et al, Effect of electron-beam irradiation on colority of printing-dyeing wastewater. J. Radiat. Res. Radiat. Process. **36**, 060401 (2018) (in Chinese). https://doi.org/10.11889/j.1000-3436.2018.rrj.36.060401.